BJRS
BRAZILIAN JOURNAL OF RADIATION SCIENCES

doi.org/10.15392/2319-0612.2024.2678
2024, 12(4B) | 01-18 | e2678
Submitted: 2024-08-30
Accepted: 2025-01-22

Development of Monte Carlo Models for Neutronic Simulation of SEALER

Duarte [a], J. Q. C.; Campagnani [a], T. O.; Pereira [a], C.; Silva [a*], C. A. M.

[a] Universidade Federal de Minas Gerais, Departamento de Engenharia Nuclear, Av. Antônio Carlos, 6627, Campus UFMG, PCA 1, Bloco 04, Anexo Engenharia, Pampulha, 31270-90, Belo Horizonte, MG, Brazil.

Corresondence: * clarysson@nuclear.ufmg.br

Abstract: This work focuses on modeling the Swedish Advanced Lead Reactor (SEALER-Artic), considering current trends in the development of Small Modular Reactors (SMRs) and the well-known advantages of lead-cooled nuclear systems. The objective of the study is to compare neutronic parameters using the following stochastic codes: Monte Carlo N-Particle, version 6.2.0 (MCNP 6.2.0), and Open Monte Carlo, version 0.14.0 (OpenMC 0.14.0). In this context, the neutron energy spectrum, the radial neutron flux profile in the reactor core, the relative power distribution, the criticality, and the fuel evolution during the burnup cycle of SEALER-Artic are evaluated. The steady-state results show good agreement of neutronic parameters between the codes. After the burnup, the final fuel composition shows a greater difference, possibly due to the nuclear data used in the decay calculation and the truncation of the atomic fraction calculation during the fuel evolution simulation.

Keywords: Small Modular Reactors, Lead-cooled Fast Reactor, SEALER-Arctic, Neutronic Simulations, MCNP 6.2.0, OpenMC 0.14.0.

SBPR

BJRS
BRAZILIAN JOURNAL OF RADIATION SCIENCES

doi.org/10.15392/2319-0612.2024.2678
2024, 12(4B) | 01-18 | e2678
Submitted: 2024-08-30
Accepted: 2025-01-22

Desenvolvimento de Modelos usando Método Monte Carlo para simulação Neutrônica do SEALER

Resumo: O presente trabalho foca na modelagem do Reator Avançado Sueco refrigerado a chumbo (SEALER-Artic), considerando as atuais tendências para o desenvolvimento de Reatores Modulares de Pequeno Porte (SMRs) e as conhecidas vantagens dos sistemas nucleares refrigerados a chumbo. O objetivo do estudo é comparar parâmetros neutrônicos utilizando os códigos estocásticos Monte Carlo N-Particle, versão 6.2.0 (MCNP 6.2.0), e Open Monte Carlo, versão 0.14.0 (OpenMC 0.14.0). Nesse contexto, avalia-se o espectro de energia dos nêutrons, o perfil radial do fluxo neutrônico do núcleo do reator, a distribuição relativa de potência, a criticalidade e a evolução do combustível durante o ciclo de queima do SEALER-Artic. Os resultados em estado estacionário apresentam boa concordância dos parâmetros neutrônicos entre os códigos utilizados. Após a queima, a composição final do combustível irradiado apresenta uma maior diferença, possivelmente devido aos dados nucleares utilizados no cálculo de decaimento e à truncagem no cálculo da fração atômica dos nuclídeos durante a simulação da evolução do combustível.

Palavras-chave: Reator Modular de Pequeno Porte, Reator Rápido Refrigerado a Chumbo, SEALER-Arctic, Simulações Nuetrônicas, MCNP 6.2.0, OpenMC 0.14.0.

SBPR

1. INTRODUCTION

Small Modular Reactors (SMRs) represent the latest proposal for generating electric power, typically up to 300 MW, and they have generated significant interest from the scientific community and enterprises. They could be used as a complement for intermittent renewable energy sources while offering streamlined systems and expedited construction. Moreover, SMRs offer enhanced passive safety, a compact size, and a long-life reactor core [1]. In this context, the Swedish Advanced Lead Reactor (SEALER), designed by LeadCold Reactors, aims to meet the demands for commercial power production in the Arctic regions of Canada. SEALER-Arctic is an 8MWt lead-cooled fast reactor that uses uranium oxide enriched to 19.75%. Its core design aims to achieve criticality with the smallest possible geometry [2][3][4].

The present work focuses on developing the SEALER-Arctic model for neutronic analysis, utilizing Monte Carlo codes due to their capability to represent detailed 3D geometries. The simulation uses OpenMC 0.14.0 and MCNP 6.2.0 to verify the agreement of neutronic parameters among these codes and the reference works, which uses SERPENT 1.18.0 code [3][4]. These models enable the evaluation of the neutronic behavior of the SEALER-Arctic under distinct operating conditions and predict its physical response. This study evaluates the effective multiplication factor (k_{eff}), shutdown margin (SDM), delayed neutron fraction (β_{eff}), relative power distribution (RPD), neutron energy spectrum, neutron flux profile, and spent fuel composition at end of life (EOL). The following sections outline the methodology applied to the simulations, compare the results of the neutronic parameters, and analyze the spent fuel composition at EOC.

2. METHODOLOGY

The SEALER-Arctic model uses available data from standard references. Reactor dimensions, material composition, and density were based on previous works [3-8]. **Figure 1** illustrates the SEALER-Arctic core, and **Table 1** presents its main features.

Table 1 : Main parameters of SEALER core [3].

DESCRIPTION	VALUE	DESCRIPTION	VALUE
Fuel assemblies	19	Burn-up control assembly rod pitch	32.92 mm
Fuel pins per assembly	91	Shut-down assemblies	6
Fuel pin pitch	16.37 mm	(W, Re)$^{10}B_2$ rods/shut-down assembly	7
Fuel pin P/D (Hot state)	1.127	Shut-down assembly rod pitch	45.00 mm
Wire space diameter	1.84 mm	Reflector assemblies	24
Thicknessof diagrid plates	50 mm	YSZ rods/reflector assembly	37
Diameter of diagrid plates	TBD	Reflector rod pitch	25.07 mm
Diagrid vertical (internal) distance	300 mm	Shield assemblies	24
Burn-up control assemblies	12	$^{10}B_4C$ rods/shield assembly	19
B_4C rods/burn-up control assembly	19	Shield assembly rod pitch	34.75 mm

Figure 1: Axial and radial view of SEALER core [2][3][4].

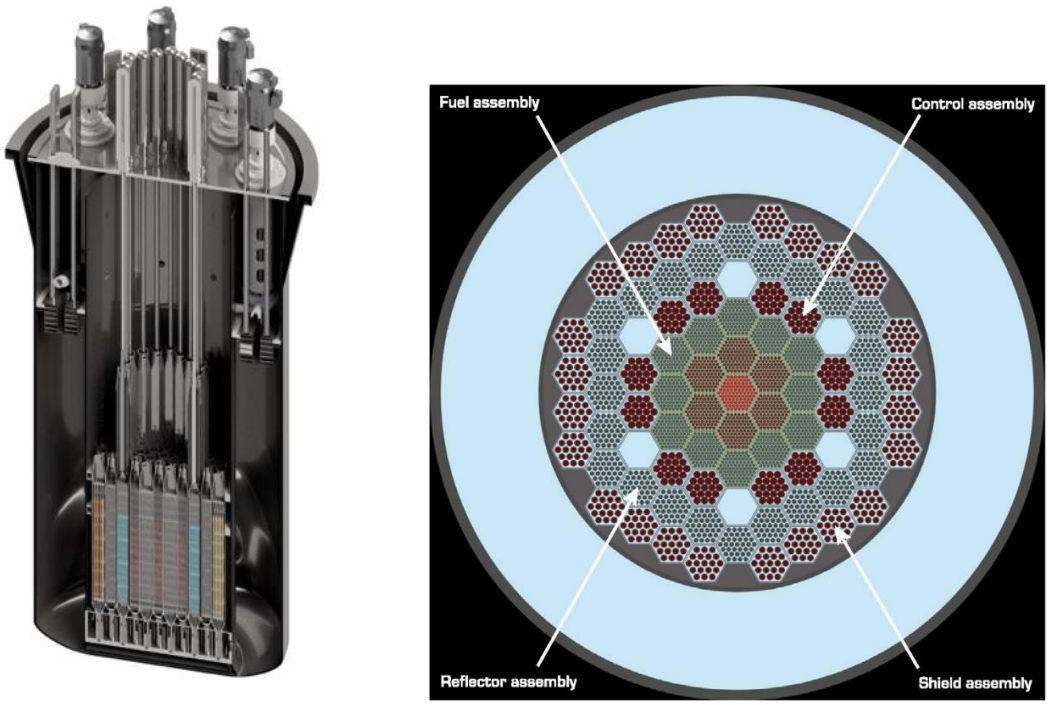

MCNP and OpenMC models are identical in terms of geometry, material composition, and density. They were configured using a 13 x 13 hexagonal lattice, with each mesh representing an assembly type, such as fuel, control, reflector or shield assembly, as shown in the design reference (**Figure 1**). Within each assembly type, there is a smaller hexagonal lattice used to configure the pin pitch distance, which is distinct for each assembly due to the different number of rods (**Table 1**). This modeling methodology results in a heterogeneous geometry for the SEALER-Arctic core, representing each assembly type with distinct rods, specific materials, and density. Furthermore, control assemblies can be gradually inserted into reactor core to adjust the reactor's reactivity. **Figure 2** illustrates the configured geometry in both codes.

Figure 2: MCNP and OpenMC model

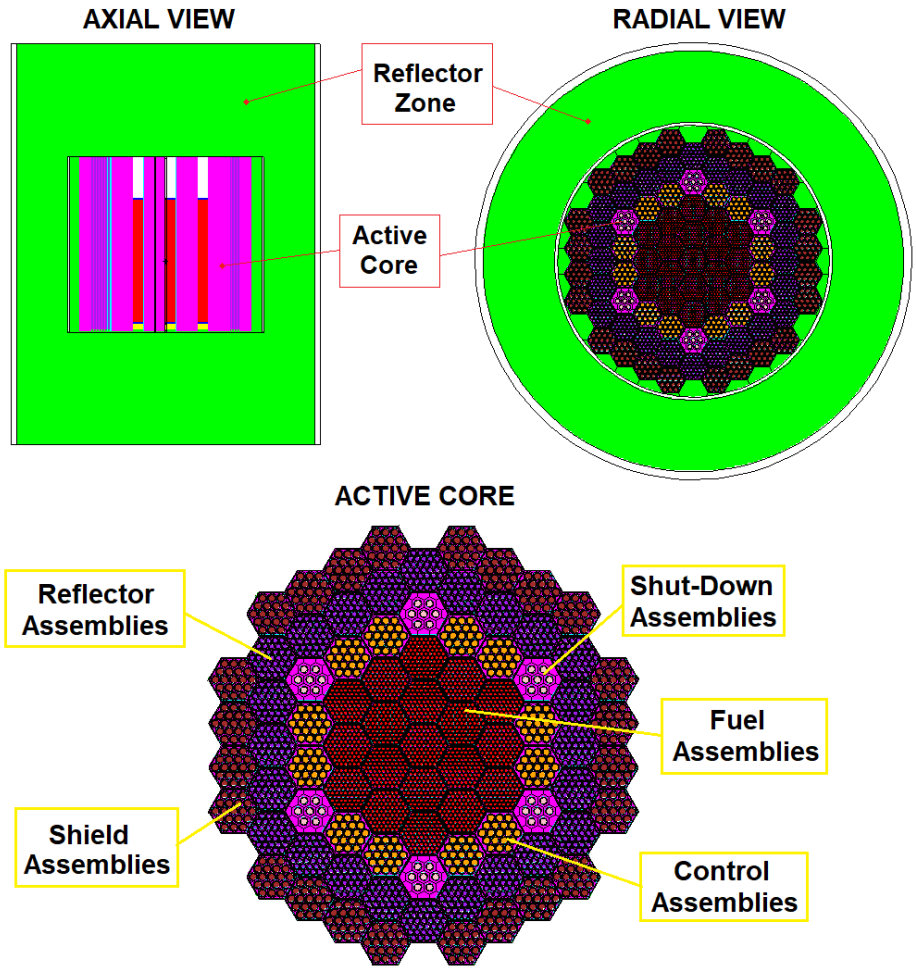

The results were derived from comprehensive full-core calculations, simulating 360 active cycles with 15,000 particles per cycle. To ensure the convergence of the fission source distribution, each simulation excluded 40 cycles before initiating active tallies. This methodology results in a maximum standard deviation of effective multiplication factor of 31 pcm, and for the neutron flux, a relative error smaller than 5.0%, as reported in the code references.

The simulations consider the operational reactor temperature: 750K for the fuel, 684K for the coolant, 690K for the fuel cladding, and 663K for the other components of the system. The nuclear data were generated using the NJOY code for the corresponding temperatures, and the MCNP and OpenMC models use the JEFF-3.1 and ENDF-B/VIII.0 libraries for comparison with reference works [3][4].

The SEALER-Arctic was designed to operate for 10 to 30 years [2-4]. Thus, aiming to verify the maximum energy generation, the burnup simulations consist of 30 Effective Full Power Years (EFPY) at a thermal power of 8.0 MW(t), which corresponds to a total of 35.20 GWd/ton(HM). In order to verify the reactivity excess during the operational reactor cycle, the simulations do not consider reactivity control, and all control rods are extracted from the core during burnup.

3. RESULTS AND DISCUSSIONS

3.1. Comparison of MCNP and OpenMC to the reference source

Stochastic codes are widely recognized for calculating neutronic parameters and providing the associated standard deviations. MCNP and OpenMC estimate values of approximately 28 pcm for k_{eff}, 38 pcm for β_{eff}, and 28 pcm for SDM. The references do not report the estimated standard deviation for SERPENT [3][4], but the calculated parameters are useful as a basis for comparison with MCNP and OpenMC. **Table 2** presents the main neutronic parameters calculated in the present study using MCNP and OpenMC, as well as

those calculated in the reference work using the SERPENT code [3][4]. The k_{eff} and β_{eff} calculations consider all control rods and shutdown rods extracted from the core. Evidently, the shutdown margin (SDM) is simulated with all of them fully inserted into the core, aiming to estimate the level of safety and assurance that the reactor will remain subcritical after a shutdown. In order to verify the impact of different nuclear data on the neutronic parameters at steady-state, the mean value ($\bar{x}$) and standard deviation (SD) were calculated using the following equations:

$$\bar{x} = \frac{\sum_1^N x_i}{N} \tag{1}$$

$$SD = \sqrt{\frac{\sum(x_i - \bar{x})^2}{N}} \tag{2}$$

where N represents the total number of values and x_i each individual parameter value. In addition, the absolute difference (AD) and relative difference (RD) were calculated with respect to the mean values of the neutronic parameters, as follows:

$$AD = |x_i - \bar{x}| \tag{3}$$

$$RD\ (\%) = \frac{AD}{x_i} \cdot 100 \tag{4}$$

Table 2 : Main neutronic paramters calculated at steady-state for SEALER-Arctic.

CODE	LIBRARY	k_{eff}	β_{eff} (pcm)	SDM (pcm)	AD			RD (%)		
					k_{eff}	β_{eff}	SDM	k_{eff}	β_{eff}	SDM
MCNP	JEFF-3.1	1.04817	747	-3053	87	6	79	0.08	0.80	2.59
	ENDF-B/VIII.0	1.04650	739	-3256	80	2	124	0.08	0.27	3.81
OpenMC	JEFF-3.1	1.04816	723	-3009	86	18	123	0.08	2.49	4.09
	ENDF-B/VIII.0	1.04653	745	-3340	77	4	208	0.07	0.54	6.23
SERPENT	JEFF-3.1	1.04712	752	-3000	18	11	132	0.02	1.46	4.40
STATISTICAL ANALYSIS	Mean Value	1.04730	741	-3132						
	SD (pcm)	74	10	140						

In **Table 2**, SERPENT presents a k_{eff} value closest to the mean, and thus its absolute difference is smaller than the standard deviation (74 pcm). For MCNP and OpenMC, the ENDF-B/VIII.0 library shows the smallest AD, with values close to the SD.

When comparing MCNP and OpenMC with SERPENT, some discrepancies are observed. Using the same library (JEFF-3.1), MCNP and OpenMC present AD values of 87 pcm and 86 pcm for k_{eff}, respectively, while SERPENT shows an AD of 18 pcm. This fact may be due to the absence of precise data used in the SERPENT simulation for the reflector material (YSZ), as well as the temperature and composition of the reactor's structural components. In the MCNP and OpenMC simulations, the composition and density of YSZ are based on general descriptions found in the literature [6]. The structural components use material specifications from experimental studies [7][8] and are modeled with a temperature corresponding to the core inlet lead temperature of 663K. Among the evaluated parameters, SDM has the highest RD, which may be due to the absence of accurate data for absorber materials in control assemblies and shut-down assemblies. However, this difference is around 6%, and according to the documentation for the codes [9-12], the accuracy is adequate to ensure that the geometry and materials are properly defined. Thus, the next phase will evaluate additional neutronic features for MCNP and OpenMC using ENDF-B/VIII.0.

3.2. Neutron flux features and relative power distribution

Figure 3 illustrates the neutron energy spectrum for both codes, demonstrating a good agreement between them. As expected, this spectrum shows a hardening effect, with the highest values in the epithermal energy range. Around 0.4 MeV, the total scattering cross-section of ^{16}O exhibits a peak, indicating the highest probability of scattering reactions occurring at this energy. Since this reaction reduces neutron energy, a decrease in the number of neutrons is expected around 0.4 MeV, resulting in a reduction in neutron flux within this energy range. In fact, **Figure 3** illustrates this behavior: the energy range with the highest total scattering cross-section of ^{16}O corresponds to a reduction in neutron

flux. Conversely, the energy range with lower scattering cross-section values shows a hardening of the neutron spectrum.

Figure 3: Neutron energy spectrum and total scattering cross-section for ^{16}O.

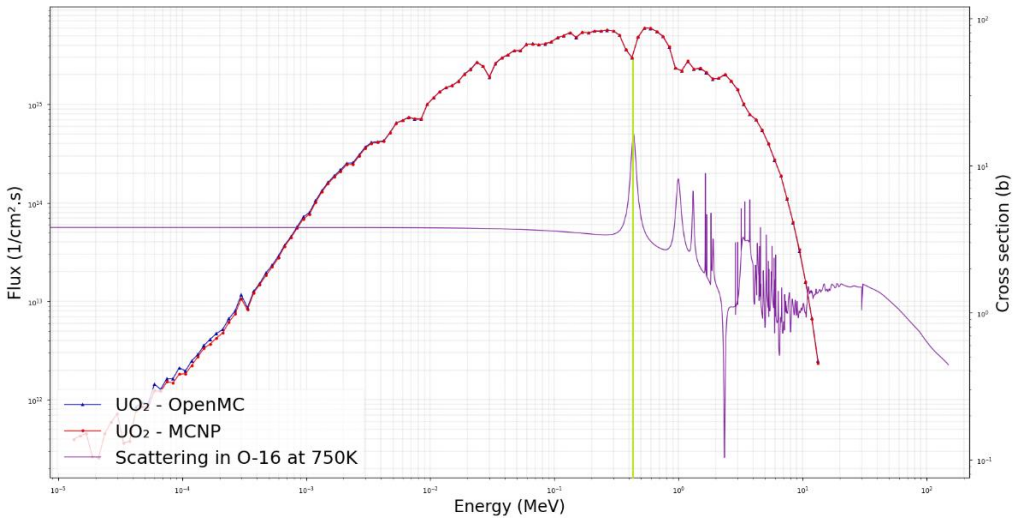

As widely presented in the literature, stochastic codes can be used to calculate the average neutron flux in a specified region. MCNP and OpenMC provide the ability to tally particles on a mesh that operates independently of the problem's geometry, while also estimating flux based on the user-defined source. In the simulated models, a cylindrical mesh was set up within the SEALER-Arctic core to calculate the neutron flux in each mesh.

Figure 4 depicts the neutron flux profile in SEALER-Arctic with all control rods and shutdown rods extracted from the core. MCNP and OpenMC exhibit very similar behavior and show good agreement in the calculated flux. Since these simulations do not include reactivity control, the neutron flux is highest in the central core zone. The axial flux profile is greater in the middle sections of the core and decreases toward the top and bottom. Similarly, the radial flux profile is highest at the core center and decreases toward the periphery. This behavior could be due to the higher concentration of fuel assemblies at core center, which leads to a greater number of fission reactions. Additionally, the presence of reflectors in the outer core zone contributes to this behavior. Neutrons that escape from the core are reflected back, resulting in a higher flux in the center.

Figure 4: Axial and radial neutron flux profiles in the reactor core.

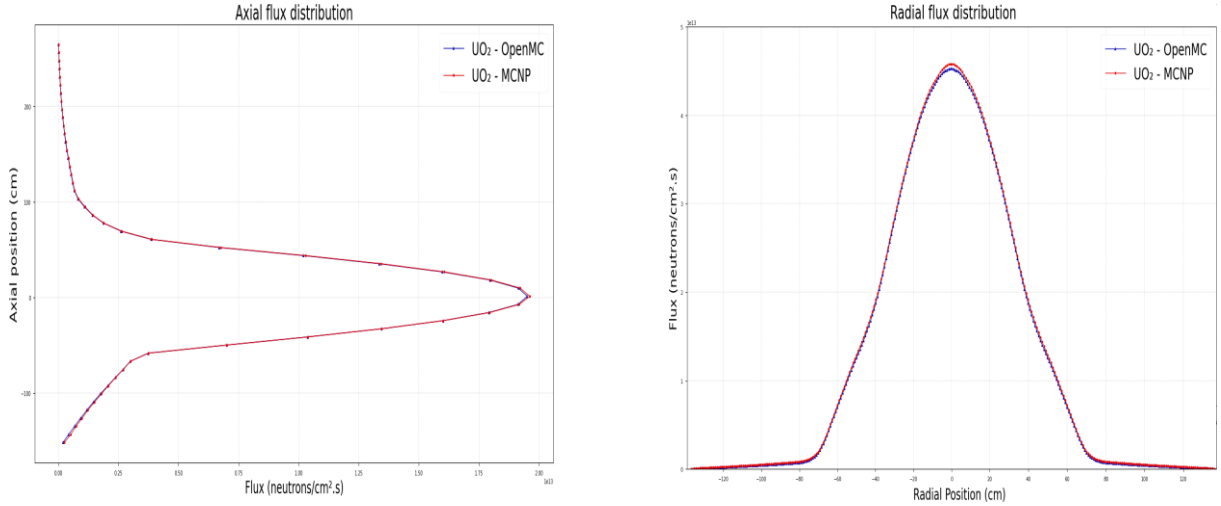

Figure 5 and **Table 3** present the results of the relative power distribution in the radial direction. As expected, these values correspond to the pattern of the axial neutron flux profile. The central fuel assembly has the highest RPD and the outer fuel assemblies present the smallest values. The neutron flux determines the rate of fission reactions, and thus the local power generated within the reactor core. Higher neutron flux results in more fission reactions, leading to higher local power generation. Conversely, regions with lower neutron flux will generate less power.

Figure 5: Radial RPD map for active core of SEALER-Arctic.

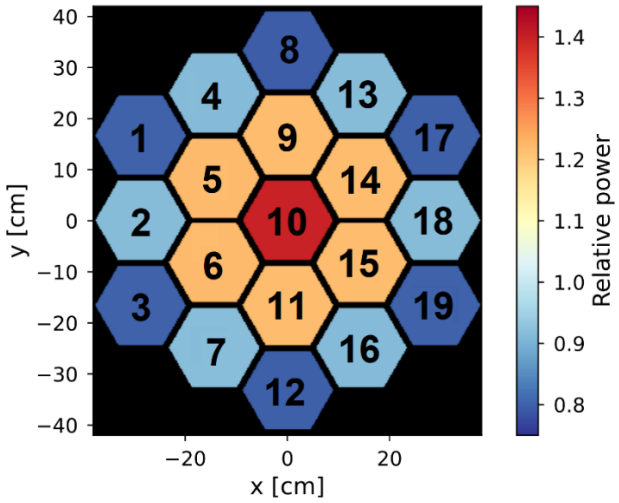

Table 3 : Radial RPD values calculated by MCNP and OpenMC.

FUEL ASSEMBLY	RPD			AD	RD	RELATIVE ERROR (%)	
	MCNP	OpenMC	MEAN			MCNP	OpenMC
1	0.8043	0.7979	0.8011	0.0032	0.3995	0.1558	0.2242
2	0.9193	0.9131	0.9162	0.0031	0.3384	0.1462	0.1885
3	0.8027	0.7996	0.8012	0.0015	0.1935	0.1558	0.2186
4	0.9173	0.9177	0.9175	0.0002	0.0218	0.1462	0.2030
5	1.2185	1.2176	1.2181	0.0005	0.0369	0.1178	0.1615
6	1.2184	1.2195	1.2190	0.0006	0.0451	0.1178	0.1669
7	0.9173	0.9153	0.9163	0.0010	0.1091	0.1462	0.2049
8	0.8009	0.8016	0.8013	0.0004	0.0437	0.1558	0.2228
9	1.2143	1.2215	1.2179	0.0036	0.2956	0.1178	0.1685
10	1.3927	1.3997	1.3962	0.0035	0.2507	0.1085	0.1414
11	1.2133	1.2202	1.2168	0.0034	0.2835	0.1178	0.1636
12	0.7990	0.7976	0.7983	0.0007	0.0877	0.1558	0.2227
13	0.9169	0.9143	0.9156	0.0013	0.1420	0.1463	0.2039
14	1.2171	1.2205	1.2188	0.0017	0.1395	0.1178	0.1528
15	1.2117	1.2199	1.2158	0.0041	0.3372	0.1178	0.1635
16	0.9123	0.9147	0.9135	0.0012	0.1314	0.1462	0.1997
17	0.8045	0.8001	0.8023	0.0022	0.2742	0.1559	0.2218
18	0.9182	0.9140	0.9161	0.0021	0.2292	0.1462	0.2060
19	0.8012	0.7955	0.7984	0.0029	0.3570	0.1558	0.2272

Table 3 shows that MCNP and OpenMC present the highest RPD at fuel assembly Nº10 and the smallest at fuel assembly Nº19. These codes show good agreement in the calculated RDP values, with a maximum Relative Difference (*RD*) about 0.4%.

Figure 6 plots the values from **Table 3**, illustrating the similar behavior of the codes with respect to RPD and relative errors calculated by the codes. The peaks in RPD correspond to fuel assemblies in the internal zone of the core (**Figure 5**), where higher values induce to lower relative error. On the other hand, higher relative errors are associated with smaller RPD values at fuel assemblies Nos. 1, 3, 8, 12, 17, and 19. They are located in the

outer core zone (**Figure 5**), where the neutron flux is lower, resulting in fewer particles in this region. This fact may be contributing to the observed behavior.

However, the highest relative error calculated by the codes is around 0.22%, indicating that MCNP and OpenMC present accurate RPD. According to the code references, this value ensures the reliability of the calculations [9-12].

Figure 6: RPD and Relative Error as a function of number of fuel assembly.

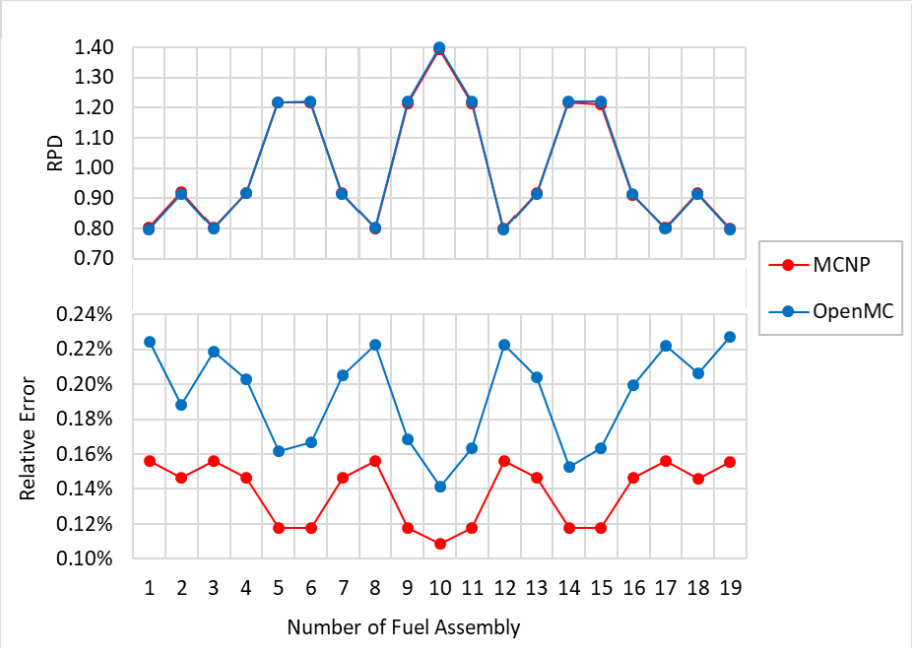

3.3. Fuel evolution during the reactor life.

As expected, the effective multiplication factor decreases during burnup, primarily due to the reduction of fissile isotopes and the increase in neutron-absorbing nuclides. The simulations show approximately a 2% decrease in the mass of fissile isotopes and about a 1% increase in fission products, including ^{127}I, ^{129}I, ^{135}I, ^{129}Xe, ^{131}Xe, ^{132}Xe, ^{134}Xe, ^{135}Xe, ^{133}Cs, ^{134}Cs, ^{135}Cs and ^{138}Ba, as well as about a 1% increase in actinides ^{234}U, ^{236}U, ^{237}U, ^{236}Np, ^{237}Np, ^{238}Np, ^{239}Np, ^{238}Pu, ^{240}Pu and ^{242}Pu. This behavior may provoke a reduction in k_{eff}, corresponding to a reactivity swing of about 4000 pcm (**Figure 7**).

Figure 7: Effective multiplication factor as a function of burnup

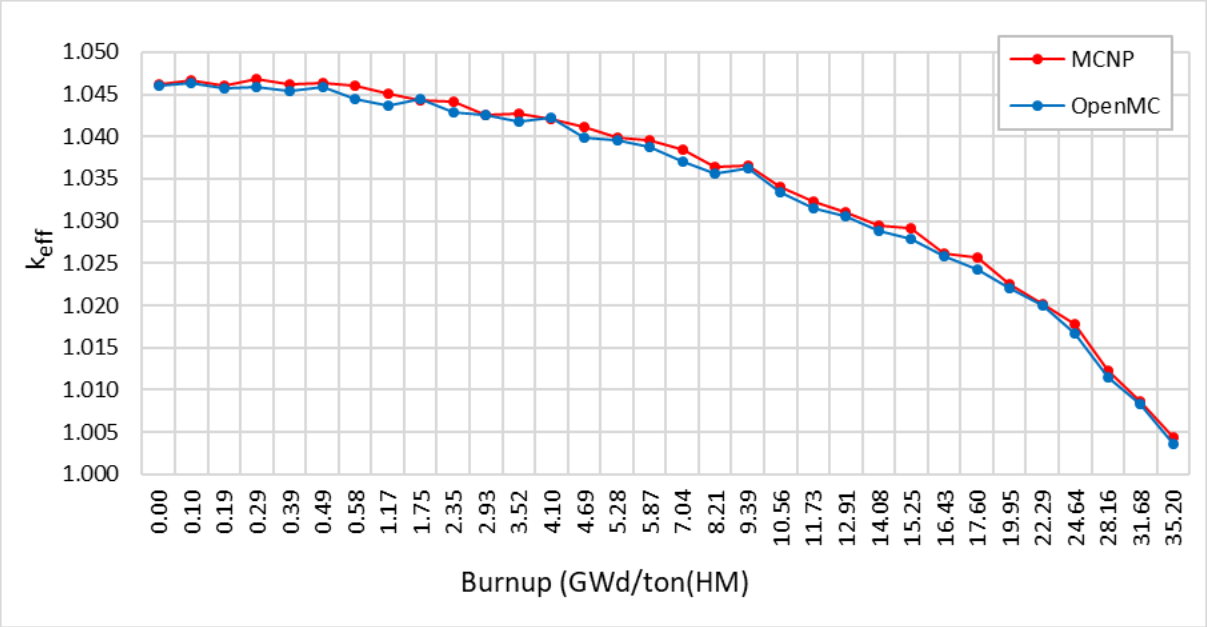

Comparing the codes, MCNP and OpenMC show good agreement in k_{eff} values and exhibit similar behavior in reactivity swing during burnup. The maximum absolute difference in k_{eff} between the codes is 157 pcm, which corresponds to 0.15%. Both codes predict that the reactor core will have positive reactivity at the end of life, with k_{eff} around 1.0040.

Table 4 presents the variation of the main actinides in the fuel composition (in atomic fraction) over 30 EFPY for SEALER-Arctic (burnup of GWd/ton(HM)). This variation was calculated as:

$$Variation = af_{EOL} - af_{BOL} \tag{5}$$

where af_{EOL} and af_{BOL} represent the atomic fractions at the end of life (EOL) and the beginning of life (BOL), respectively. The mean value, absolute difference (AD), and relative difference (RD) were calculated using the previous equations (2), (3), and (4).

Both codes show the same behavior in isotopic fuel variation. As expected, they present a reduction in ^{235}U and ^{238}U, and an increase in the other isotopes (**Table 4**). The

fission of ^{235}U causes its decrease over time, while the radioactive capture of ^{238}U is the main process that contributes to its reduction. This reaction produces isotopes of Np and Pu, which increase during burnup. Additionally, ^{234}U may be produced by alpha decay from ^{238}Pu, and capture reactions of ^{235}U could produce ^{236}U and ^{237}U. Therefore, the used codes present the same behavior

Table 4 : Variation in fuel composition (atom fraction) during the burnup.

Nuclide	CODE	BOL	EOL	Variation	Mean Value	AD	RD
^{234}U	OpenMC	0.00E+00	8.56E-06	8.56E-06	8.42E-06	1.46E-07	2%
	MCNP	0.00E+00	8.27E-06	8.27E-06		1.46E-07	2%
^{235}U	OpenMC	6.65E-02	5.28E-02	-1.37E-02	-1.35E-02	2.24E-04	2%
	MCNP	6.65E-02	5.32E-02	-1.33E-02		2.24E-04	2%
^{236}U	OpenMC	0.00E+00	2.67E-03	2.67E-03	2.62E-03	5.04E-05	2%
	MCNP	0.00E+00	2.57E-03	2.57E-03		5.04E-05	2%
^{237}U	OpenMC	0.00E+00	1.37E-07	1.37E-07	1.32E-07	4.80E-09	4%
	MCNP	0.00E+00	1.27E-07	1.27E-07		4.80E-09	4%
^{238}U	OpenMC	2.67E-01	2.58E-01	-8.63E-03	-8.51E-03	1.15E-04	1%
	MCNP	2.67E-01	2.58E-01	-8.40E-03		1.15E-04	1%
^{237}Np	OpenMC	0.00E+00	9.16E-05	9.16E-05	8.83E-05	3.23E-06	4%
	MCNP	0.00E+00	8.51E-05	8.51E-05		3.23E-06	4%
^{238}Np	OpenMC	0.00E+00	3.64E-09	3.64E-09	3.43E-09	2.04E-10	6%
	MCNP	0.00E+00	3.23E-09	3.23E-09		2.04E-10	6%
^{239}Np	OpenMC	0.00E+00	2.06E-06	2.06E-06	2.01E-06	4.39E-08	2%
	MCNP	0.00E+00	1.97E-06	1.97E-06		4.39E-08	2%
^{238}Pu	OpenMC	0.00E+00	4.78E-06	4.78E-06	4.51E-06	2.65E-07	6%
	MCNP	0.00E+00	4.25E-06	4.25E-06		2.65E-07	6%
^{239}Pu	OpenMC	0.00E+00	5.69E-03	5.69E-03	5.57E-03	1.22E-04	2%
	MCNP	0.00E+00	5.45E-03	5.45E-03		1.22E-04	2%
^{240}Pu	OpenMC	0.00E+00	1.09E-04	1.09E-04	1.04E-04	4.91E-06	5%
	MCNP	0.00E+00	9.93E-05	9.93E-05		4.91E-06	5%
^{241}Pu	OpenMC	0.00E+00	1.12E-06	1.12E-06	1.05E-06	7.34E-08	7%
	MCNP	0.00E+00	9.74E-07	9.74E-07		7.34E-08	8%
^{242}Pu	OpenMC	0.00E+00	1.34E-08	1.34E-08	2.18E-08	8.40E-09	63%
	MCNP	0.00E+00	3.02E-08	3.02E-08		8.40E-09	28%

Since MCNP and OpenMC use the same model, they have identical fuel compositions at the beginning of life (BOL). However, at EOL, there are discrepancies in the atomic

fraction of the evaluated nuclides, which may be associated with truncation in the burnup calculations and or different nuclear data for nuclide decay. Although both codes use the similar chain decay reactions and the same neutron library, the default setting in MCNP6.2.0 excludes nuclides with atomic fractions below 1.0E-10 to reduce computational time. Thus, nuclides with atomic fractions below this threshold are set to zero in the depletion calculations and are removed from further processing after the initial time point. In addition, both codes incorporate detailed information about decay modes, but they may handle this data differently based on their specific functionalities.

Among the evaluated isotopes, ^{242}Pu exhibits the highest relative difference (RD) (**Table 4**). Considering that ^{242}Pu is produced from the radioactive capture of ^{241}Pu, the nuclear data for the chain decay of plutonium isotopes may differ between the codes, or these data might be processed differently. Another hypothesis could be related to MCNP truncation. OpenMC includes Pu, Np, Am, and Cm isotopes with atomic fractions below 1.0E-10, which are not accounted for in MCNP. This discrepancy may be contributing to the observed differences in behavior. However, for other nuclides, the relative differences are smaller than 9%.

4. CONCLUSIONS

The results demonstrate the capability of MCNP 6.2.0 and OpenMC 0.14.0 to model detailed geometry systems. The simulations present accurate results consistent with previous studies using the SERPENT 1.18.0 code. Among these codes, the largest relative difference is observed in the shut-down margin. Comparing the neutronic parameters calculated by MCNP 6.2.0 and OpenMC 0.14.0, they show closely matching values demonstrating consistency and appropriate modeling at steady state. During the burnup, MCNP and OpenMC present similar criticality and comparable reactivity swing. However, the spent fuel

composition after 30 EFPY present larger discrepancies, which may be vinculated to specif depletion process of the used codes. For more accurate results, it is essential to use consistent nuclear data for nuclide decay, identical decay chains in the calculations, and the same truncation order for atomic fractions of nuclides in burnup calculation. The present work indicates that MCNP 6.2.0 and OpenMC 0.14.0 are suitable for modeling a small lead-cooled reactor. However, the depletion results highlight the need for consistent data in the decay processes and decay chain reactions. In this sense, to validate a depletion methodology in MCNP and OpenMC, it is necessary to compare the burnup results with those from other widely recognized codes in the field of nuclear engineering. Therefore, future studies will use the Oak Ridge Isotope GENeration (ORIGEN) code to accomplish this goal. Considering its extensive international use by nuclear regulatory bodies, research institutions, and commercial entities, this code can contribute to research on small lead-cooled systems.

ACKNOWLEDGMENT

The authors are grateful to the Brazilian research funding agencies, CNPq (Brazil), CAPES (Brazil), FAPEMIG (MG/Brazil) and CNEN (Brazil), for the support.

CONFLICT OF INTEREST

All authors declare that they have no conflicts of interest.

REFERENCES

[1] IAEA. Technology roadmap for small modular reactor deployment / International Atomic Energy Agency. Vienna, Austria, 2021.

[2] WALLENIUS, J.; QVIST, S.; MICKUS, I.; BORTOT, S.; EJENSTAM, J.; SZAKALOS, P. SEALER: A small lead-cooled reactor for power production in the Canadian Arctic. *In*: INTERNATIONAL CONFERENCE ON FAST REACTORS AND RELATED FUEL CYCLES: NEXT GENERATION NUCLEAR SYSTEMS FOR SUSTAINABLE DEVELOPMENT (FR17) 2017, Yekaterinburg, Russian Federation, Proceedings Series - International Atomic Energy Agency , IAEA, Vienna, 2018.

[3] WALLENIUS, J.; QVIST, S.; MICKUS, I.; BORTOT, S.; SZAKALOS, P.; EJENSTAM, J. Design of SEALER, a very small lead-cooled reactor for commercial power production in off-grid applications, **Nuclear Engineering and Design**, v. 338, p. 23-33, 2018.

[4] WALLENIUS, J.; BORTOT, S.; MICKUS, I. Unprotected transients in Sealer: a small lead-cooled reactor for commercial power production in Arctic regions. *In*: PROCEEDINGS OF PHYSICS OF REACTORS. INTERNATIONAL CONFERENCE (PHYSOR 2018). REACTOR PHYSICS PAVING THE WAY TOWARDS MORE EFFICIENT SYSTEMS 2018, Cancun, Mexico. Sociedad Nuclear Mexicana

[5] WALLENIUS, J. Shutdown Rod for Lead-cooled Reactors. Patent Cooperation Treaty publication WO 2017/105325 A1, 2017.

[6] YOSHITO, W. K.; USSUI, V.; LAZAR, D. R. R.; PASCOAL, J. O. A. Synthesis and Characterization of NiO-8YSZ Powders by Coprecipitation Route. **Materials Science Forum**, v. 498, p. 612–617, 2005.

[7] EJENSTAM, J.; HALVARSSON, M.; WEIDOW, J.; JÖNSSON, B.; SZAKALOS, P. Oxidation studies of Fe10CrAl–RE alloys exposed to Pb at 550°C for 10,000h. **Journal of Nuclear Materials**, v. 443, p. 161-170, 2013.

[8] BANERJEE, A.; RAJU, S.; DIVAKAR, R.; MOHANDAS, E.; PANNEERSELVAM, G.; ANTONY, M. P. Thermal property characterization of a titanium modified austenitic stainless steel (alloy D9). **Journal of Nuclear Materials**, v. 347, p. 20-30, 2005.

[9] GOORLEY, J. T.; JAMES, M. R.; BOOTH, T. E.; BROWN, F. B.; BULL, J. S.; COX, L. J.; DURKEE JR., J. W.; ELSON, J. S.; FENSIN, M. L.; FORSTER III, R. A.; HENDRICKS, J. S.; HUGHES III, H. G.; JOHNS, R. C.; KIEDROWSKI, B. C.; MARTZ, R. L.; MASHNIK, S. G.; MCKINNEY, G. W.; PELOWITZ, D. B.; PRAEL, R. E.; SWEEZY, J. E.; WATERS, L. S.; WILCOX, T.; ZUKAITIS, A.J. Initial MCNP6 Release Overview - MCNP6 version 1.0. Los Alamos National Laboratory. Report LA-UR-13-22934 (USA), 2013.

[10] ROMANO, P. K.; HORELIK, N. E.; HERMAN, B. R.; NELSON, A. G.; FORGET, B.; SMITH, K. OpenMC: A State-of-the-Art Monte Carlo Code for Research and Development. **Annals of Nuclear Energy**, v. 82, p. 90-97. 2015.

[11] ROMANO, P. K.; HERMAN, B. R.; HORELIK, N. E.; FORGET, B.; SMITH, K.; SIEGEL, A. R. Progress and Status of the OpenMC Monte Carlo Code. *In*: PROCEEDING OF INTERNATIONAL CONFERENCE ON MATHEMATICS AND COMPUTATIONAL METHODS APPLIED TO NUCLEAR SCIENCE AND ENGINEERING, Sun Valley, Idaho, 2013.

[12] ROMANO, P. K.; FORGET, B. The OpenMC Monte Carlo Particle Transport Code. **Annals of Nuclear Energy**, v. 51, p. 274-281, 2013.

LICENSE